Deformed one-quasiparticle states in covariant density functional theory

A.V. Afanasjev *, S. Shawaqfeh [1]

Department of Physics and Astronomy, Mississippi State University, MS 39762, United States

ARTICLE INFO

ABSTRACT

Systematic investigation of the accuracy of the description of the energies of deformed one-quasiparticle states has been performed in covariant density functional theory in actinide and rare-earth mass regions. The sources of the discrepancies between theory and experiment are analyzed. Although some improvements in the description of ground state configurations and one-quasiparticle spectra can be achieved by better parametrization of the relativistic mean field Lagrangian, the analysis suggests that spectroscopic quality of their description can be achieved only in theoretical framework which takes into account particle–vibration coupling.

© 2011 Elsevier B.V. Open access under CC BY license.

1. Introduction

Further progress in understanding low energy nuclear phenomena in stable and exotic nuclei is strongly connected with the development of nuclear density functional theory (DFT) in its non-relativistic and relativistic (covariant) incarnations. These theories provide rather successful description of different aspects, such as deformations, masses, collective excitations, etc., of nuclear many-body problem, see Refs. [1,2] and references therein. In addition, they are aimed on global (i.e. across full nuclear chart) description of the nuclear properties.

However, absolute majority of the applications of nuclear DFT has been focused on collective properties of nuclei. This is due to the fact that time-odd mean fields are needed for the description of one-(many)-particle configurations which are characterized by broken time-reversal symmetry in intrinsic frame (see Ref. [2] and references therein). As a result, the description of such configurations is more complicated as compared with the one of the ground states of even–even nuclei.

There are only few features of deformed nuclear systems, strongly dependent on single-particle degrees of freedom, which have been addressed in the DFT studies on the mean-field level and compared with experiment. When discussing the impact of single-particle degrees of freedom on nuclear properties, it is important to separate different aspects of their physics which only weakly depend on each other. These are (i) deformation polarization effects induced by particle or hole, (ii) alignment properties of single-particle orbital in rotating potential and relevant polarization effects in time-odd mean fields, and (iii) the single-particle energies.

Let us consider each of those aspects. The addition of the particle to (or the creation of the hole in) even–even core induces deformation polarization effects. The investigation of superdeformed rotational bands in the $A \sim 140$–150 mass region, which are one of the best examples of undisturbed single-particle motion [3,4], has revealed that deformation polarization effects induced by particle or hole are well described in non-relativistic [3,5] and covariant [5,4] DFT's; the average deviation from available experimental differential quadrupole moments is around 20%. Similar (but somewhat less accurate because of the role of pairing) results have been obtained also in the $A \sim 130$ mass region of high- and superdeformation [6,7]. Macroscopic + microscopic (MM) method based on the Nilsson potential describes deformation polarization effects reasonably well but suffers from the fact that these effects are not uniquely defined [8,9].

Alignment properties of single-particle orbital in rotating potential can be accessed via effective (relative) alignments [10] of two compared rotational bands. This quantity sensitively depends on both the alignment properties of single-particle orbital by which two bands differ and polarization effects (mostly in time-odd mean fields) induced by the particle in this orbital [11]. Effective alignments are on average better reproduced in the covariant DFT (CDFT) calculations than in the cranked Nilsson–Strutinsky version

---

* Corresponding author.
E-mail address: afansjev@erc.msstate.edu (A.V. Afanasjev).
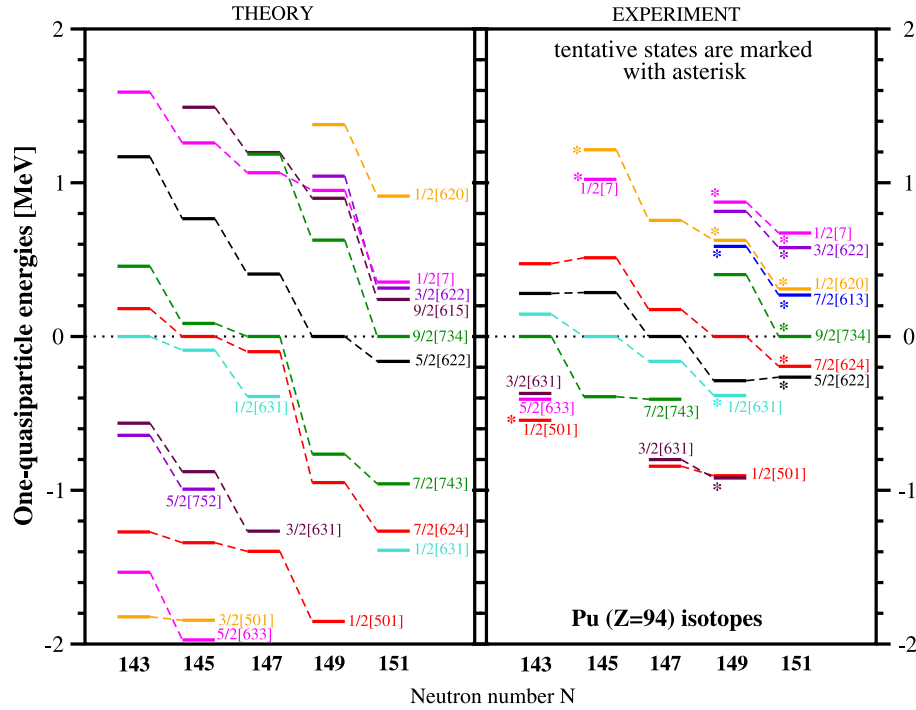[1] Deceased.

Fig. 1. The evolution of one-quasineutron energies as a function of neutron number for the Pu isotopes. Hole states are plotted below the ground state (zero energy), and particle states are plotted above. Experimental data (one-quasineutron band-head energies) are taken from Ref. [32]. The squared amplitudes of the dominant component of the wave function change gradually with neutron number. Thus, their variations are presented below in the neutron number range where these states are plotted in left panel in the following format: [state label: A–B], where A is the squared amplitude of the dominant component of wave function at lower value of N and B at upper value of N. These variations are 1/2[501]: 0.67–0.46, 3/2[501]: 0.82–0.87, 5/2[752]: 0.57–0.56, 5/2[633]: 0.77–0.78, 3/2[631]: 0.55–0.57, 7/2[743]: 0.72–0.74, 1/2[631]: 0.58–0.51, 5/2[622]: 0.65–0.69, 7/2[624]: 0.86–0.89, 7/2[613]: 0.78–0.83, 3/2[622]: 0.66–0.52, 9/2[615]: 0.96–0.96, 9/2[734]: 0.82–0.85. The 1/2[7] state is strongly mixed. However, the cumulative squared amplitude of the components of the wave function with $N = 7$ in the structure of this state exceeds 90%. Thus, we label it only by principal quantum number N and Ω.

of the MM approach based on phenomenological Nilsson potential, see comparisons presented in Refs. [11–13]. Reasonable description of effective alignments can be obtained also in Skyrme DFT [9,14], but it is somewhat plagued by the uncertainties in the definition of the coupling constants for time-odd mean fields [14,15]. This problem does not exists in the CDFT since time-odd mean fields are defined via Lorentz covariance [2].

The discussion above clearly shows that some aspects of the single-particle motion are described on average better and in a more consistent way in self-consistent DFT than in phenomenological MM method. This is despite the fact that no single-particle information (apart of some spin-orbit splittings in the case of Skyrme DFT) has been used in the fit of the DFT parameters, while the parameters of the Nilsson or Woods–Saxon potentials are fitted to experimental single-particle energies (see, for example, Refs. [16–20]). However, starting from earlier studies of the single-particle spectra of few nuclei in actinides within covariant [21] and Skyrme DFT [22], and following by later global survey of the ground state configurations in odd-mass nuclei (Ref. [23]) and the investigations of the spectra of odd-proton Ho nuclei (Fig. 6 in Ref. [15]) in triaxial Skyrme DFT and the spectra of selected Rb [24], Y and Nb [25] nuclei in axial Gogny DFT [25], it became clear that the single-particle spectra are poorly described with modern DFT. It is obvious that these theories do not possess spectroscopic quality description of the single-particle spectra which is achievable in the MM method as a consequence of the fit of the potential parameters to experimental single-particle energies.

Despite these results, no systematic analysis of the accuracy of the description of the single-particle spectra has been performed in DFT. The current manuscript aims on such analysis within the

CDFT using extensive set of experimental data on the energies of one-quasiparticle states in deformed nuclei. There are two main goals behind of this study. First, typical uncertainties in the description of single-particle energies will be defined. Second, the sources of discrepancies and possible ways of the improvement of the description of the single-particle spectra will be discussed.

2. The details of calculations

Cranked relativistic Hartree–Bogoliubov (CRHB) approach is used in the current manuscript in a similar way as it was done in an earlier study of the spectra of few odd-mass actinide nuclei in Ref. [21]. Time-odd mean fields are taken into account, and the blocking due to odd particle (see Section VI.A in Ref. [21] for details) is performed in a fully self-consistent way. The D1S Gogny force is used in the pairing channel. Nuclear configurations of deformed odd nuclei (further one-quasiparticle [1-qp] configurations) are labeled by means of the asymptotic quantum number $\Omega[Nn_z\Lambda]$ (Nilsson quantum number) of the dominant component of the wave function of blocked single-particle orbital. In each nucleus under study, the binding energies are calculated for a number of the 1-qp configurations based on the orbitals active in the vicinity of the Fermi level, and then the 1-qp spectra are built as shown in Fig. 1.

The CRHB equations are solved in the basis of an anisotropic three-dimensional harmonic oscillator in Cartesian coordinates. The same basis deformation $\beta_0 = 0.3$, $\gamma = 0°$ and oscillator frequency $\hbar\omega_0 = 41A^{-1/3}$ MeV have been used for all nuclei. All fermionic and bosonic states belonging to the shells up to $N_F = 14$ and $N_B = 18$ are taken into account in the diagonalization of the

Table 1

The summary of calculations. The number of calculated 1-qp configurations and the number of experimental 1-qp states compared with calculations are displayed in second and third columns, respectively. Fourth column gives the percentage of ground states, the structure of which is correctly reproduced in the calculations.

Region (parametrization)	Calculated states (#)	Compared states (#)	Correct ground states (%)
Actinides (NL3*)	415	209	38%
Actinides (NL1)	444	217	45%
Rare-earth (NL1)	360	149	48%

Dirac equation and the matrix inversion of the Klein–Gordon equations, respectively. The comparison with the results of calculations in a larger fermionic basis ($N_F = 16$) shows that the energies of quasiparticle states are described with an accuracy of approximately 50 keV which is sufficient for a statistical analysis.

The calculations have been performed with the NL1 [26] and NL3* [27] parameterizations of the relativistic mean field (RMF) Lagrangian. The NL1 parametrization has been fitted to the nuclei in the valley of β-stability. On the contrary, the fit of the NL3* parametrization includes neutron-rich nuclei so it is partially tailored toward the description of such nuclei. This recently fitted parametrization has been successfully applied to the description of binding energies [27], ground state properties of deformed nuclei [28], spectra of odd spherical nuclei within the relativistic particle–vibration model [30], rotating nuclei [27], giant resonances [27], and breathing mode [31]. Note that only bulk properties of nuclei such as binding energies, radii, etc. and nuclear matter properties have been used in the fit of these two parameterizations.

1-qp spectra were calculated for 44 nuclei, namely, 21 odd-N and 23 odd-Z nuclei in actinide region with $Z = 89$–100. The nuclei with octupole deformation have been excluded from consideration. In addition, the calculations have been performed in rare-earth region. However, the experimental data on 1-qp states in rare-earth region are significantly larger than in actinide region [32]. As a consequence, the calculations were performed only for odd-proton $Z = 61$ (Pm), 63 (Eu), 65 (Tb), 67 (Ho) and 69 (Tm) isotope chains and only with the NL1 parametrization of the RMF Lagrangian; in total, for 31 odd-proton nuclei. All these nuclei are deformed with quadrupole deformation $\beta_2 \geqslant 0.2$ and labeling of their single-particle states by means of the Nilsson quantum numbers is commonly accepted [33–38]. Table 1 provides the summary of these calculations. The data on adopted experimental one-quasiparticle levels are taken from Ref. [32].

3. Statistical analysis

Fig. 1 shows the comparison of calculated and experimental one-quasineutron spectra in Pu isotopes. A number of features are clearly seen. First, for a given 1-qp state the discrepancy between theory and experiment depends on neutron number. Second, for a given 1-qp state the slope of the energy curve as a function of neutron number is more pronounced in the calculations than in experiment. These two features are interconnected and they emerge from the fact that theoretical energy scale is more stretched out than experimental one due to low effective mass (see discussion below). The change of the Fermi energy with neutron number leads to the changes of the energy differences between ground and excited states and these differences are affected by effective mass in the calculations. Third, the relative energies of different experimental 1-qp states are not always reproduced in calculations. This feature originates from the fact that the energies of spherical subshells, from which deformed states emerge, can deviate from experiment [21]. These three features are seen in all isotone and isotope chains.
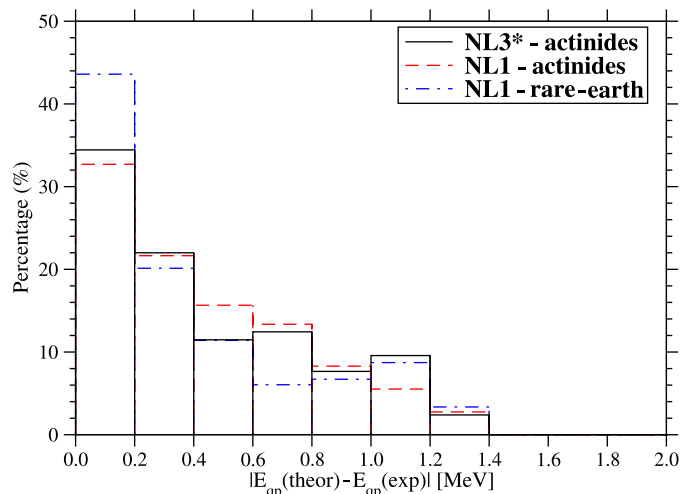

Fig. 2. The distribution of the deviations of the calculated energies E_{qp}(theor) of one-quasiparticle states from experimental ones E_{qp}(exp). The vertical axis shows the percentage of the states which deviate from experiment by the energy deviation range (the width of bar) specified on horizontal axis.

Note however that for a given state the 1-qp energy changes as a function of particle number are appreciably smaller when 1-qp energies of proton (neutron) subsystem are shown as a function of neutron (proton) number (see, for example, Fig. 6 in Ref. [15]) because the changes in proton (neutron) Fermi energy and deformation are relatively small.

Statistical analysis of the discrepancies between calculated and experimental energies of one-quasiparticle states is presented in Fig. 2. One can see that in the actinide region only approximately 33% of one-quasiparticle states are described with an accuracy better than 200 keV, and approximately 22% with an accuracy between 200 and 400 keV. The percentage of states for a given range of deviations goes gradually down with an increase of the deviation between experiment and calculations. However, for some states the deviation of calculated energy from experimental one exceeds 1 MeV and can be close to 1.4 MeV. Note that earlier analysis of the single-particle spectra of few actinide nuclei in Ref. [21] shows similar features. Fig. 2 also shows that with the NL1 parametrization the 1-qp energies in odd-proton rare-earth nuclei are somewhat better described as compared with actinide region. For example, the energies of 44% of the states are described with an accuracy better than 200 keV. Otherwise, the distribution histograms for the deviations are similar in both regions and for both parameterizations.

Fourth column of Table 1 shows the percentage of the ground states, the structure of which is correctly reproduced in the calculations. These values are comparable or somewhat better than the ones obtained in systematic Hartree–Fock + BCS calculations of deformed nuclei with SIII, SkM* and SLy5 Skyrme forces and FRDM calculations employing phenomenological folded-Yukawa potential [23], which show the agreement with experiment at about 40% level.

It is interesting that the overall accuracy of the description of the energies of deformed one-quasiparticle states is slightly better in old NL1 parametrization, which was fitted 25 years ago mostly to the nuclei at the β-stability line, than in the recent NL3* parametrization. This suggests that the inclusion of extra information on neutron rich nuclei into the fit of the NL3* parametrization may lead to some degradation of the description of single-particle states along the valley of β-stability.
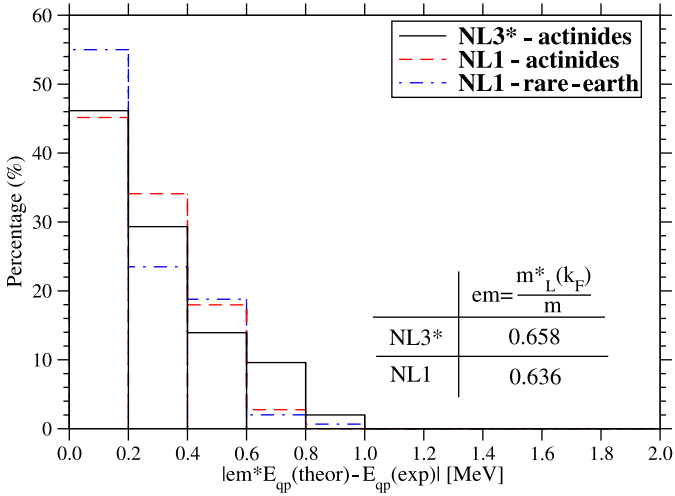
Fig. 3. The same as Fig. 2, but for the case when the energy scale of theoretical spectra is corrected for low Lorentz effective mass.

4. The sources of the discrepancies between theory and experiment

4.1. Effective mass

Low effective mass of CDFT is one of the sources of the discrepancies between theory and experiment. This is because the average level density of the single-particle states on the mean field level is related to the effective mass $m_L^*(k_F)/m$ (Lorentz mass in the notation of Ref. [39] for the case of CDFT) of the nucleons at the Fermi surface which depends on momentum as [39]

$$\frac{m_L^*(k_F)}{m} = \sqrt{\left(\frac{m^*(0)}{m}\right)^2 + \left(\frac{k_F}{m}\right)^2}$$
$$\approx \sqrt{\left(\frac{m^*(0)}{m}\right)^2 + 0.08} \qquad (1)$$

where $m^*(0)/m$ is the value at $k = 0$ which is called Dirac effective mass [39] and 0.08 is obtained for $(k_F/m)^2$ when typical value $k_F \approx 1.35$/fm is used. The values of Lorentz effective mass for employed parameterizations are given in Fig. 3.

Low effective mass leads to a stretching of theoretical single-particle energy scale as compared with experiment (see Refs. [29, 30] for comparisons of calculated and experimental spectra in spherical nuclei). The role of the energy stretching due to low effective mass can be illustrated on the example of the $\pi 1/2[420]$, $\pi 3/2[411]$ and $\pi 5/2[402]$ states in rare-earth region. These states emerge from the $\pi d_{5/2}$ spherical subshell. For the majority of the nuclei under study, the $\pi 3/2[411]$ state is located close to the proton Fermi level. As a consequence, it is observed in 25 nuclei, and its energy in those nuclei is described in the calculations with an average accuracy of 250 keV. On the contrary, the $\pi 1/2[420]$ ($\pi 5/2[402]$) state is located significantly below (above) the Fermi level both in experiment and calculations. However, stretching of theoretical energy scale due to low effective mass results in systematic deviations of calculated energies of these states from experiment by more than 1 MeV. This leads to a peak in distribution histogram of the deviations of calculated energies from experimental ones at the deviation energy of around 1.1 MeV (see Fig. 2). Another contributor to this peak is the $\pi 9/2[514]$ state.

This stretching is also clearly visible when single-particle Nilsson diagrams obtained in the CDFT and phenomenological Nilsson or Woods–Saxon potentials are compared (see, for example,

Fig. 1 in Ref. [12]). These potentials are characterized by an effective mass $m^*(k_F)/m \approx 1.0$ which gives calculated level density close to experiment. As illustrated in spherical nuclei, the calculated level density and single-particle spectra are compressed and come closer to experimental ones when CDFT is supplemented by particle–vibrational coupling (PVC) [29,30] (similar effect exists also in the PVC models based on non-relativistic DFT [40–42]).

Similar compression of calculated spectra is expected also in deformed nuclei. However, no PVC model based on DFT framework has been developed so far for such nuclei. Systematic comparison of single-particle Nilsson diagrams obtained in the CDFT and phenomenological Nilsson potential suggest that on average expected compression of the single-particle spectra can be achieved by multiplying the energies of the 1-qp configurations by Lorentz effective mass. Such energy rescaling follows also from the results of phenomenological scheme of Ref. [43] based on a linear ansatz for the energy dependence of the scalar and vector components of the nucleon self-energy for the states close to the Fermi surface which simulates the dynamical effects that arise from the coupling of single-nucleon motion to collective surface vibrations.

The impact of such energy rescaling on the distribution of the deviations between theory and experiment is shown in Fig. 3. One can see that more than 75% of states are described with an accuracy better than 400 keV; this is a typical accuracy of the description of the energies of the deformed 1-qp states within phenomenological potentials [36,44]. Although this energy rescaling is somewhat schematic, it clearly indicates that PVC, leading to an increase of effective mass [29], will also improve the description of experimental spectra as compared with mean field results; this has already been seen in spherical nuclei [30].

4.2. Relative energies of different states

Incorrectly calculated relative energies of different states (see Fig. 1) represent another source of the discrepancies between theory and experiment (see discussion of the Pu isotope chain above). It originates from the fact that relative energies of different spherical subshells, from which deformed states emerge, are not properly reproduced in model calculations [21]. This source shows up also in a statistical analysis. For example, the energy of the hole $\nu 1/2[501]$ state in actinide region is systematically higher than experimental one by around 1 MeV in both employed parameterizations. This is only deformed state originating from the $\nu p_{1/2}$ spherical subshell, so the current analysis suggests that in the calculations it is placed too deep (by approximately 1 MeV) with respect of other spherical subshells.

5. Consequences for spectroscopic quality energy density functionals

The need for quantitative understanding and highly accurate description of nuclear structure phenomena is a driving force behind the efforts to develop spectroscopic quality energy density functionals (EDF). Such efforts are especially visible in the field of non-relativistic Skyrme DFT [15,46]. However, the basic question whether this is possible on the mean-field level is still under debate [45].

It is well known from Skyrme DFT that EDF, forced to describe accurately single-particle spectra on the mean-field level, are characterized by effective mass close to one [47]. In the CDFT, one cannot improve the description of the single-particle spectra by increasing effective mass since all CDFT parameterizations on the Hartree level have Lorentz effective mass $m_L^*(k_F)/m$ close to 0.65 [2]. The current analysis for deformed nuclei strongly suggests that further progress in improving spectroscopic quality of

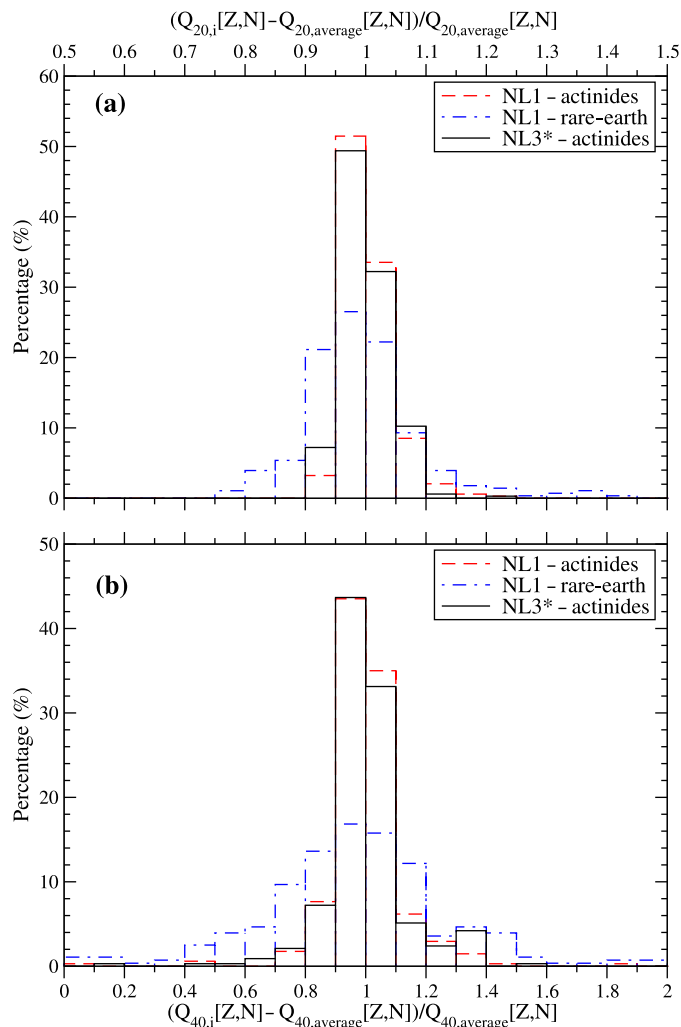**Fig. 4.** Histogram of differences between the moment of the ith 1-qp configuration and the average moment of all calculated 1-qp configurations in the (N, Z) nucleus. The distributions for mass quadrupole (panel (a)) and mass hexadecapole (panel (b)) moments are shown.

covariant EDF will be quite limited on the mean-field level. We expect that even for other modern CDFT parameterizations, not employed in the current manuscript, the distributions of the deviations of calculated energies from experimental ones of the 1-qp states will be comparable or only slightly better than the one seen in Fig. 2. This is due to their low Lorentz effective masses and unavoidable errors in relative placement of specific single-particle orbitals. However, for some parameterizations such as NLSH and NL-RA1 obtained distributions can be even worse than that of Fig. 2; this follows from the analysis of Ref. [21].

As a consequence, the only way to substantially improve the description of the single-particle properties in the framework based on CDFT is to take into account PVC. It was already illustrated in spherical nuclei that this leads to a significant improvement in the description of the experimental energies of the dominant single-particle states [29,30]. In addition, it takes care of well-known fragmentation of the single-particle strength of the levels; this feature is completely ignored on the mean-field level. Based on experience in spherical nuclei, one can expect that the inclusion of PVC in deformed nuclei will bring Lorentz effective mass close to one, thus leading to a level density which is similar to experimental one. This will definitely improve the description of the 1-qp spectra. The corrections to the energies of single-particle

states due to PVC are strongly state-dependent in spherical nuclei [29,30]. On the contrary, in deformed odd nuclei the corrections to the energies of 1-qp states due to PVC are expected to be less state-dependent since surface vibrations are more fragmented in deformed nuclei than in spherical ones [38].[2] However, they can still affect the relative energies of different deformed 1-qp states.

6. Deformation effects

Each blocked single-particle orbital induces deformation polarization effects. Fig. 4 shows the distribution of the mass quadrupole and hexadecapole moments of the 1-qp configurations relative to the respective average moments of the full set of 1-qp configurations in a given nucleus. This figure clearly shows that actinide nuclei are reasonably rigid since polarization effects (especially for quadrupole moments) induced by odd particle do not lead to substantial deviations of equilibrium moments from average values. On the contrary, rare-earth nuclei are considerably softer than actinides since their histograms are significantly wider. The results for actinides show also that polarization effects do almost not depend on the parametrization of the RMF Lagrangian; small differences between histograms obtained in the NL1 and NL3* parameterizations are most likely due to slightly different sets of the 1-qp configurations obtained in the calculations. These changes in the moments/deformations and relevant changes in the binding energies of the 1-qp configurations induced by odd particle have to be taken into account when experimental data are compared with the results of the calculations. However, they are completely ignored in the models most frequently used for the analysis of the spectra of deformed odd nuclei such as MM model [44], particle + rotor [37] and quasiparticle–phonon [38] models; these models assume the same deformation for all 1-qp states in the nucleus under study.

The calculations suggest that the deformation driving effects induced by odd proton or neutron are sufficient to polarize the nucleus toward positive or negative γ-deformation in some one-quasiparticle configurations. On average, only 6.8% of calculated states have γ-deformation in the range $1° \leqslant |\gamma| \leqslant 17°$; the γ-deformation of other states is either exactly zero (in the majority of the cases) or below $1°$. It turns out that the appearance of sizable γ-deformation correlates with blocking of few specific single-particle states. For example, in the actinide region 43% of triaxial configurations has the dominant $\nu[622]3/2$ structure, and 38% has the $\nu[501]1/2$ structure. Time-odd mean fields have almost no effect on the equilibrium deformations similar to previous CDFT studies. On the contrary, the results of Skyrme EDF studies of Ref. [15] show that the inclusion of time-odd mean fields favors the axial deformation of calculated configurations.

7. Conclusions

In conclusion, for the first time a systematic analysis of the accuracy of the description of the energies of one-quasiparticle configurations in deformed odd nuclei has been performed in the DFT framework. It provides theoretical estimates on the errors in calculated energies of one-quasiparticle configurations. Two sources of inaccuracies, namely, low effective mass leading to a stretching of the energy scale and incorrect relative positions of some single-particle states exist in model calculations. While the solution of the latter problem can be attempted in the DFT framework, we do not believe that it will lead to significant improvements in spec-

---

[2] This provides extra justification for the energy scaling procedure employed in Section 4.1.

troscopic quality of energy density functionals. The comprehensive solution requires taking into account particle–vibration coupling which will (i) compress the calculated one-quasiparticle spectra bringing them closer to experiment and (ii) correct the relative energies of different single-particle states. In our opinion, only such approach combined with respective re-parametrization of the RMF Lagrangian can lead to spectroscopic quality energy density functionals.

In addition, our results show that one should be extremely careful in the interpretation (predictions) of (for) the data which involves absolute or relative energies of different one-/two-/many-quasiparticle states since their energy description is associated with non-negligible theoretical errors. Extra care has to be taken also in the case when physical phenomenon sensitively depends on the single-particle energies. For example, the existence of very shallow left and right chiral minima with depth of around 200 keV separated by a tiny barrier (≈ 60 keV) is responsible for chiral rotation [48]. Theoretical errors in the description of single-particle energies can either create false minima (barrier) or kill real ones.

Acknowledgement

References

[1] M. Bender, P.-H. Heenen, P.-G. Reinhard, Rev. Mod. Phys. 75 (2003) 121.
[2] D. Vretenar, A.V. Afanasjev, G.A. Lalazissis, P. Ring, Phys. Rep. 409 (2005) 101.
[3] W. Satuła, J. Dobaczewski, J. Dudek, W. Nazarewicz, Phys. Rev. Lett. 77 (1996) 5182.
[4] A.V. Afanasjev, G.A. Lalazissis, P. Ring, Nucl. Phys. A 634 (1998) 395.
[5] D. Nisius, et al., Phys. Lett. B 392 (1997) 18.
[6] R.W. Laird, et al., Phys. Rev. Lett. 88 (2002) 152501.
[7] M. Matev, A.V. Afanasjev, J. Dobaczewski, G.A. Lalazissis, W. Nazarewicz, Phys. Rev. C 76 (2007) 034304.
[8] L.B. Karlsson, I. Ragnarsson, Nucl. Phys. A 639 (1998) 654.
[9] N. El Aouad, et al., Nucl. Phys. A 676 (2000) 155.
[10] I. Ragnarsson, Nucl. Phys. A 557 (1993) c167.
[11] A.V. Afanasjev, P. Ring, Phys. Scripta T 88 (2000) 10.
[12] A.V. Afanasjev, I. Ragnarsson, P. Ring, Phys. Rev. C 59 (1999) 3166.
[13] A.V. Afanasjev, S. Frauendorf, Phys. Rev. C 71 (2005) 064318.
[14] J. Dobaczewski, J. Dudek, Phys. Rev. C 52 (1995) 1827.
[15] N. Schunck, J. Dobaczewski, J. McDonnell, J. Moré, W. Nazarewicz, J. Sarich, M.V. Stoitsov, Phys. Rev. C 81 (2010) 024316.
[16] T. Bengtsson, I. Ragnarsson, Nucl. Phys. A 436 (1985) 14.
[17] D. Galeriu, D. Bucurescu, M. Ivaşku, J. Phys. G 12 (1986) 329.
[18] J. Dudek, T. Werner, J. Phys. G 4 (1978) 1543.
[19] J. Dudek, A. Majhofer, J. Skalski, T. Werner, S. Cwiok, W. Nazarewicz, J. Phys. G 5 (1978) 1359.
[20] S. Cwiok, J. Dudek, W. Nazarewicz, J. Skalski, T. Werner, Comput. Phys. Comm. 46 (1987) 379.
[21] A.V. Afanasjev, T.L. Khoo, S. Frauendorf, G.A. Lalazissis, I. Ahmad, Phys. Rev. C 67 (2003) 024309.
[22] M. Bender, P. Bonche, T. Duguet, P.-H. Heenen, Nucl. Phys. A 723 (2003) 354.
[23] L. Bonneau, P. Quentin, P. Möller, Phys. Rev. C 76 (2007) 024320.
[24] R. Rodriguez-Guzman, P. Sarriguren, L.M. Robledo, Phys. Rev. C 82 (2010) 061302(R).
[25] R. Rodriguez-Guzman, P. Sarriguren, L.M. Robledo, Phys. Rev. C 83 (2011) 044307.
[26] P.-G. Reinhard, M. Rufa, J. Maruhn, W. Greiner, J. Friedrich, Z. Phys. A 323 (1986) 13.
[27] G.A. Lalazissis, S. Karatzikos, R. Fossion, D. Pena Arteaga, A.V. Afanasjev, P. Ring, Phys. Lett. B 671 (2009) 36.
[28] Z.Q. Sheng, Z.Z. Ren, W.Z. Hang, Nucl. Phys. A 832 (2010) 49.
[29] E. Litvinova, P. Ring, Phys. Rev. C 73 (2006) 044328.
[30] E.V. Litvinova, A.V. Afanasjev, Phys. Rev. C 84 (2011) 014305.
[31] T. Gaitanos, A.B. Larionov, H. Lenske, U. Mosel, Phys. Rev. C 81 (2010) 054316.
[32] Evaluated Nuclear Structure Data File (ENSDF) located at the website (http://www.nndc.bnl.gov/ensdf/) of Brookhaven National Laboratory. ENSDF is based on the publications presented in Nuclear Data Sheets (NDS) which is a standard for evaluated nuclear data. Adopted experimental one-quasiparticle levels are taken from the NDS articles published during 2001–2011.
[33] A. de Shalit, H. Feshbach, Theoretical Nuclear Physics, vol. I (Nuclear Structure), John Wiley & Sons, New York, London, Sydney, Toronto, 1974.
[34] A. Bohr, B.R. Mottelson, Nuclear Structure, vol. 2, Benjamin, New York, 1975.
[35] R.R. Chasman, I. Ahmad, A.M. Friedman, J.R. Erskine, Rev. Mod. Phys. 49 (1977) 833.
[36] A.K. Jain, R.K. Sheline, P.C. Sood, K. Jain, Rev. Mod. Phys. 62 (1990) 393.
[37] S.G. Nilsson, I. Ragnarsson, Shapes and Shells in Nuclear Structure, Cambridge University Press, 1995.
[38] V.G. Soloviev, Theory of Atomic Nuclei: Quasiparticles and Phonons, Institute of Physics Publishing, Bristol, Philadelphia, 1992.
[39] M. Jaminon, C. Mahaux, Phys. Rev. C 40 (1989) 354.
[40] P. Quentin, H. Flocard, Ann. Rev. Nucl. Part. Sci. 28 (1978) 523.
[41] C. Mahaux, P.F. Bortignon, R.A. Broglia, C.H. Dasso, Phys. Rep. 120 (1985) 1.
[42] G. Coló, H. Sagawa, P.F. Bortignon, Phys. Rev. C 82 (2010) 064307.
[43] D. Vretenar, T. Nikšić, P. Ring, Phys. Rev. C 65 (2002) 024321.
[44] A. Parkhomenko, A. Sobieczewski, Acta Phys. Polon. 35 (2004) 2447.
[45] P.F. Bortignon, G. Coló, H. Sagawa, J. Phys. G 37 (2010) 064013.
[46] M. Zalewski, J. Dobaczewski, W. Satuła, T.R. Werner, Phys. Rev. C 77 (2008) 024316.
[47] B.A. Brown, Phys. Rev. C 58 (1998) 220.
[48] V.I. Dimitrov, S. Frauendorf, F. Dönau, Phys. Rev. Lett. 84 (2000) 5732.